

AJTE99-6148

FIRE SUPPRESSION EFFICIENCY SCREENING USING A COUNTERFLOW CYLINDRICAL BURNER

JIANN C. YANG, MICHELLE K. DONNELLY, NIKKE PRIVE, AND WILLIAM L. GROSSHANDLER
Building and Fire Research Laboratory
National Institute of Standards and Technology
Gaithersburg, Maryland 20899, U.S.A.
tel 301-975-6662; FAX 301-975-4052; jiann.yang@nist.gov

Keywords: *Halon Replacement, Agent Screening, Counterflow burner*

ABSTRACT

The design and validation of a counterflow cylindrical burner for fire suppression efficiency screening are described. The stability limits of the burner were mapped using various fuel (propane) and oxidizer (air) flows. The stability envelopes compared favorably with those reported in the literature. The apparatus was characterized using inert gases (argon, helium, and nitrogen), and the relative fire suppression efficiency ranking of these three gases was found to be commensurate with that from cup-burner tests. For liquid suppression experiments, a piezoelectric droplet generator was used to form droplets ($< 100 \mu\text{m}$). Water was used as a representative liquid suppressant to study the feasibility of using such a burner for screening liquid agents. Extinction was facilitated with the addition of water droplets, and the effect of water became more pronounced when its application rate was increased. Suppression experiments using water with and without nitrogen dilution in the oxidizer stream were also performed. Flame extinction due to the combined effect of water and nitrogen dilution was demonstrated.

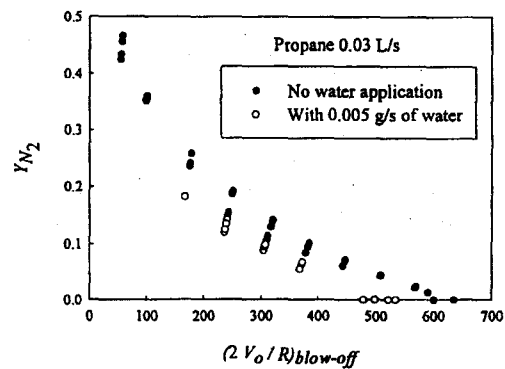


Figure A-1 Mass fraction of nitrogen added in air as a function of stagnation velocity gradient at blow-off

INTRODUCTION

The recent ban on halon 1301 (CF₃Br) production (as a result of its ozone depleting potential) has resulted in extensive search for its replacements and alternatives. Potential uses of liquid agents as replacements have been recently proposed in several applications (e.g., shipboard machinery spaces, engine compartments in armored vehicles). The applications of fire suppression efficiency screening methods constitute an important aspect of this search process because good screening methods can facilitate the identification, comparison, and selection of potential candidates for halon replacement. Most of the current screening methods (e.g., cup burners) are designed for evaluating fire suppressing agents that are delivered in the form of vapor although they have been occasionally used for evaluating condensed-phase agents (e.g., sodium bicarbonate powder, Grosshandler *et al.*, 1994). Currently there is no apparatus designed specifically for screening liquid agents; therefore, there is a need for the development of a reliable screening method for liquid agents that can be delivered in droplet form. The objective of our work is to design, construct, and demonstrate a laboratory-scale apparatus that can perform the screening of liquid agents in a well-controlled experimental setting. The design of the apparatus is based on a well-characterized flame, a means to facilitate the introduction of small amount of liquid agents, and a way to generate liquid droplets that can be entrained into the flame. These individual components will be described in detail in the following sections.

Since a porous cylindrical burner in a counterflow configuration has been extensively used to study flame structure (Tsuji and Yamaoka, 1967; 1969; 1971, Tsuji, 1982) and flame extinction using inert gases (Ishizuka and Tsuji, 1981) and halons (Milne *et al.*, 1970), it is logical to extend the application of such a burner configuration to liquid fire suppressants. In our liquid agent screening apparatus, we make use of such a burner wherein a diffusion flame is formed in the forward stagnation region of the burner placed in a uniform oxidizer flow, with fuel being ejected uniformly from the burner surface. Other counterflow geometry has recently been used for extinction studies with water aerosols (Fleming *et al.*, 1998).

There are many advantages associated with the use of a counterflow cylindrical burner. The fuel and the oxidizer flows can be independently adjusted, if required. The flame is laminar, two-dimensional, and very stable in the forward stagnation region. The geometry of the burner and the flow field allow for relatively simple analysis of the forward stagnation region (Dixon-Lewis *et al.*, 1984; Dreier *et al.*, 1986; Peters and Kee, 1987; Olson and T'ien, 1987; Dixon-Lewis and Missaghi, 1988; Chen and Weng, 1990; Sick *et al.*, 1990). Both wake and enveloped flames can be easily maintained over a wide range of fuel and oxidizer flows. The flame is easily observed, and critical stages such as the blow-off limit (abrupt transition from an enveloped flame to a wake flame) can be ascertained with ease and high reproducibility. The flame front can be easily accessed by intrusive (Tsuji and Yamaoka, 1969;

1971) or non-intrusive (Dreier *et al.*, 1986; Sick *et al.*, 1990) probing techniques, thus enabling detailed studies of flame structure.

EXPERIMENTAL APPARATUS

Burner

The design of the burner is based on several important criteria. The burner has to be robust, easily built, installed, and operated, and able to generate reliable screening test data.

The burner is a *replaceable* porous (20 μm) sintered stainless steel standard $\frac{1}{2}$ " UNF threaded cup filter with a length of 3.18 cm (1.25"), an i.d. of 1.12 cm (0.44"), and an o.d. (D) of 1.58 cm (0.625"). The advantage of this burner design over those used in the past is that burner replacement can be easily performed if partial or complete clogging of the porous burner surface occurs. The burner is screwed onto an extended insert through which fuel is injected into the interior of the porous filter and double-pass cooling water runs. The cooling water is used to cool the burner (to prevent damage to

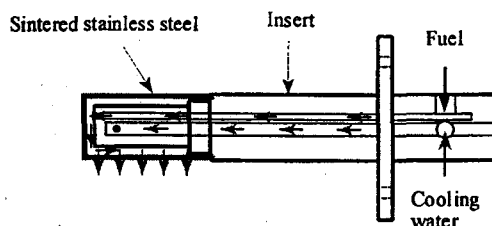


Figure 1 Cross sectional view of burner

the porous surface structure) and the fuel (to prevent fuel pyrolysis prior to its ejection through the porous surface). A cross sectional schematic of the burner interior is shown in Figure 1.

The burner, together with the insert, does not completely span the entire test section of the wind tunnel. A cylindrical brass rod (same diameter as the burner) with internal water cooling is inserted from the opposite wall and is used as an extension so that the burner assembly can be treated as a single cylinder across the test section.

The rearward 180° of the burner surface is coated with a thin layer of high-temperature resistant black paint in order to prevent fuel ejection into the wake region. The high pressure drop across the porous sintered surface assures a very uniform fuel flow over the burner surface, thus the fuel ejection velocity (V_f) is calculated by dividing the fuel volumetric flow rate by the available fuel ejection area of the burner surface.

Propane is used as fuel, and its flow rate is regulated by a mass-flow controller which is controlled by a personal computer. A bubble flow meter was used to calibrate the mass-flow controller.

Flow Facility

A small-scale vertically upward open-circuit wind tunnel is used to provide oxidizer (air) flow to the burner. The tunnel, except the test section, is made of clear polycarbonate for visual observation of droplet transport toward the burner. The tunnel consists of a blower, a diffuser, a flow straightener, a contraction section, and a test section where the burner is placed in cross-flow. This configuration not only allows for the delivery of a uniform flow of oxidizer to the burner at a low turbulence intensity but also assists in the delivery of liquid agent droplets to the flame. Figure 2 is a photograph of the flow facility.

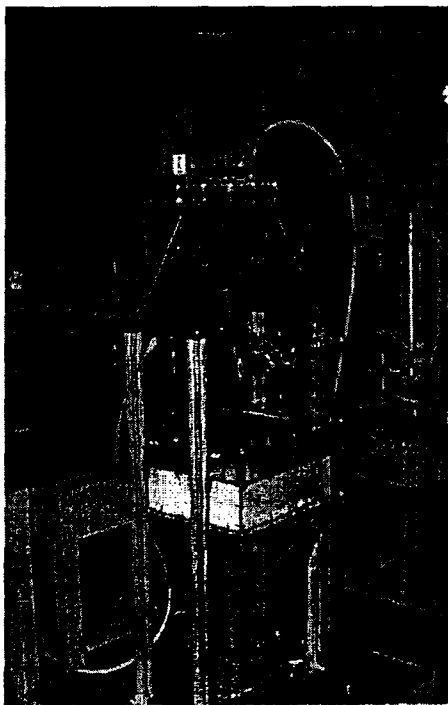


Figure 2 Photograph of flow facility

The air flow in the tunnel is provided by a variable-speed (frequency controlled) blower, whose outlet is connected to the main part of the wind tunnel via a flexible aluminum tube and a coupling to convert a circular cross section to a square. The blower was calibrated using a pitot probe equipped with a differential pressure transducer capable of measuring up to 133 Pa. In the measurements, the pitot-static tube was placed in the location where the burner would be mounted. The velocity profile obtained was relatively flat ($< \pm 0.5\%$) except in the region near the walls (boundary layers). Due to the limited frequency response of the pitot tube, the turbulent intensity level was not measured; however, the observation of a very stable laminar flame zone in the forward stagnation region of the burner provided a qualitative indication of low turbulent intensity. The volumetric flow rates are calculated using the

measured average velocities (V_o) and the cross sectional area of the test section.

The diffuser is 30 cm long, with an inlet cross sectional area of 10 cm x 10 cm and an expansion ratio (based on areas) of 1:9. The flow straightener consists of a polycarbonate honeycomb with cell diameter of 0.32 cm (0.125") and a 50 mesh stainless steel screen with 30.3 % open area. The contraction section with a contraction ratio (based on areas) of 9:1 has an inlet cross sectional area of 30 cm x 30 cm and is 30 cm long. A square flange, which was machined to have a smooth transition passage to minimize flow separation, is placed between the outlet of the contraction section and the inlet of the test section. The test section has a cross sectional area of 10 cm x 10 cm and a length of 20 cm. It is made of anodized aluminum with three Pyrex[®] observation windows (12 cm x 7 cm x 0.64 cm) flushly mounted on the three walls of the test section using high-temperature silicone RTV[®]. The burner is inserted through the fourth wall. The combustion products from the burner are vented to an exhaust hood.

Droplet Generator

One of the most important steps in the liquid suppressant screening is to be able to deliver the liquid agent in droplet form to the flame zone to cause suppression or extinction. A droplet generator is used in the proposed screening in lieu of a spray because all the droplets, in principle, can be directed to the flame zone, thus minimizing droplet loss to the wall of the flow facility caused by the fan-out of a spray. In addition, the application of a spray may require more agent to perform a test than using a droplet generator, which may not be ideal or feasible for some potential new liquid agents that can only be synthesized in minute quantity.

The droplet generator is based on the following well-established liquid jet break-up theory. According to Rayleigh's analysis of the instability of capillary jets, the frequency f for maximum instability is given by the following equation (Bayvel and Orzechowski, 1993):

$$f = \frac{u_j}{4.508 d_j} \quad (1)$$

where u_j is the jet velocity and d_j is the jet diameter. When the jet is perturbed at this frequency, uniform sized droplets with uniform spacing are formed. Rayleigh's analysis is based on an inviscid liquid jet. Experimentally, mono-dispersed droplets can be generated within a range of frequencies (Schneider and Hendricks, 1964):

¹Certain commercial products are identified in this paper in order to specify adequately the equipment used. Such identification does not imply recommendation by the National Institute of Standards and Technology, nor does it imply that this equipment is the best available for the purpose.

$$\frac{u_j}{7 d_j} < f < \frac{u_j}{35 d_j} \quad (2)$$

Depending on the droplet generator design, an extension of the above frequency range has been reported (Warnica *et al.*, 1991). The droplet diameter, D_d , resulting from the controlled jet break-up can be calculated from the jet velocity and the imposed disturbance frequency using a simple mass balance, assuming the droplet mass is equivalent to that of a jet cylinder of length u_j / f and jet diameter d_j .

$$D_d = \left(\frac{6 Q}{\pi f} \right)^{1/3} \quad (3)$$

where Q is the volumetric flow rate of the jet. For a given flow rate, the droplet diameter can be varied by changing the perturbation frequency.

In our experimental apparatus, a piezoelectric transducer driven at a fixed frequency (10 kHz) was used as a means to control the break-up of a liquid jet to form uniform droplets ($< 100 \mu\text{m}$).

The design of the droplet generator is similar to that described in Yang *et al.* (1997). The droplet generator consists of a liquid chamber which is connected to a reservoir, a bleed port (for eliminating any air bubbles trapped inside the chamber during priming), a $25 \mu\text{m}$ sapphire orifice mounted on a set screw, and a piezoelectric transducer. The initial jet emanating from the orifice is obtained by pressurizing the liquid reservoir with nitrogen. Jetting from the orifice can be achieved with very low nitrogen pressurization ($\sim 0.03 \text{ MPa}$). A $0.5 \mu\text{m}$ filter is used in the liquid feedline to minimize clogging of the orifice opening due to potential foreign particulates in the liquid.

The droplet generator is located in the settling chamber and is approximately 42 cm upstream of the burner. The presence of the droplet generator in the wind tunnel does not create any significant perturbation or blockage effect on the oxidizer flow field near the burner because the flame characteristics do not change with or without the presence of the droplet generator in the flow stream. Although uniform size droplets with uniform spacing are observed several centimeters ($\sim 10 \text{ cm}$) from the orifices as a result of controlled jet break-up, the droplet behavior becomes random further downstream, which may be due to the wake and drag effects on the droplets in the stream. The air stream in the wind tunnel also facilitates the dispersion of the single droplet stream into a small droplet cloud. By adjusting the location of the droplet generator with respect to the burner, droplet loss to the wind tunnel walls can be eliminated or minimized because the resulting dispersed droplet cloud is confined to a very narrow region near the burner.

Distilled and de-ionized water was used as a representative liquid agent to evaluate the feasibility of the proposed screening apparatus. Experiments with nitrogen addition to the air stream were also performed.

RESULTS AND DISCUSSION

Validation of Burner Performance

The first step to evaluate the test facility was to ensure that the burner functioned properly. This was achieved by mapping out the flame stability diagram of the burner and by observing flame behavior consistent with that described in Tsuji and Yamaoka (1967; 1969). There are two important parameters, fuel ejection velocity (V_f) and oxidizer velocity (V_o) in the wind tunnel, that govern the performance of the burner.

Under certain flow conditions, a thin, laminar, two-dimensional blue flame is established at a distance in front of the cylinder surface. An example is given in Fig. 3(a). As the fuel ejection velocity is decreased or the air velocity is increased, the flame slowly approaches the cylinder surface, and eventually the flame is abruptly blown off from the stagnation region, and a wake flame, an example of which is shown in Fig. 3(b), is established. Conversely, with increasing fuel velocity or decreasing air velocity, the flame zone gradually moves away from the cylinder surface, and eventually a laminar two-dimensional flame can no longer be sustained.

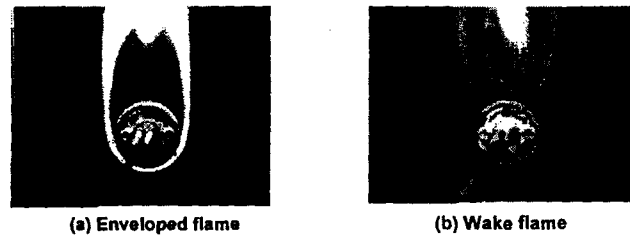


Figure 3 Examples of two flame modes

When the air velocity is very small and the fuel velocity is large, the flame zone becomes thicker, and an inner luminous yellow and an outer blue zone appear. When the air velocity is very large and reaches a critical value, the flame can never be stabilized, irrespective of the fuel ejection velocity.

Figure 4 shows the various flame stability regions of the burner obtained from the test facility. The abscissa is expressed as $2V_o/R$ (R being the burner radius) because this term represents the stagnation velocity gradient (Tsuji and Yamaoka, 1967) and has the unit of strain rate (s^{-1}). Each data point in solid circle was obtained by increasing the fuel flow rate at a fixed oxidizer flow until a luminous yellow zone appeared. The conditions above these data points represent the existence of a yellow luminous zone. The data points in solid triangles represent the blow-off limit. Each data point was obtained by increasing the oxidizer flow at a fixed fuel ejection velocity until blow-off occurred. The conditions below the blow-off limit indicate the existence of a wake flame. However, the oxidizer flow will eventually reach a limiting or critical value as the fuel injection velocity increases. From Figure 4, this critical blow-off $(2V_o/R)_{critical}$ is $\sim 615 \text{ s}^{-1}$.

sectional area of the chamber. If the initial droplet velocity is small, it is likely that the droplet (depending on its initial size) will not be entrained upwards by the low-speed air, and the droplet will eventually fall down due to gravity. The desirable droplet size for the experiments can be estimated by using the equation of motion for a droplet.

$$m \frac{dV_d}{dt} = 3\pi\mu_o D_d f_d (V_o - V_d) + mg - \frac{\rho_o g m}{\rho_d} \quad (4)$$

where m is the droplet mass, V_d is the droplet velocity, t is the time, μ_o is air viscosity, f_d is the drag factor, g is the gravitational acceleration, ρ_o is air density, and ρ_d is droplet density. For $Re_r \leq 10^5$, the drag factor can be obtained from (Crowe *et al.*, 1998)

$$f_d = 1 + 0.15 Re_r^{0.687} + \frac{0.0175}{(1 + 4.25 \times 10^4 Re_r^{-1.16})} \quad (5)$$

where $Re_r = \frac{D_d |V_o - V_d| \rho_o}{\mu_o}$

Using the above two equations, the worse-case experimental design scenario, which would likely be $V_d = 0$ and $V_o = 0.5 V_{o,critical} \times (1/9)$, is examined. The assumption that the burner is operating at half of the critical velocity is made, and the air velocity at the settling chamber is one-ninth of that at the test section (based on the 9:1 contraction area ratio). Figure 7 shows the calculated droplet velocity as a function of time with three droplet sizes. The calculations were obtained by using $V_{o,critical} = 2.4$ m/s. Negative droplet velocity indicates that the droplet is falling and cannot be entrained upwards by the existing air flow. Since the orifice size used in the experiments is 25 μm , the droplets generated should be less than 75 μm from Eqs. (1) and (3). In addition, the non-zero initial droplet velocity and the acceleration of the air as it travels into the contraction section will facilitate the droplet delivery into the burner.

Figure 8 shows the mass fraction of water added as a function of $2V_o/R$ at blow-off. Extinction tests were performed by gradually increasing the air flow until blow-off occurred at a fixed water flow. The mass fraction of water was calculated by

$$Y_{H_2O} = \frac{\dot{m}_{H_2O}}{\dot{m}_{H_2O} + \dot{m}_O} \quad (6)$$

where \dot{m}_{H_2O} is the mass flow rate of water and \dot{m}_O is the mass flow rate of oxidizer. As shown in Fig. 8, it is easier to blow-off

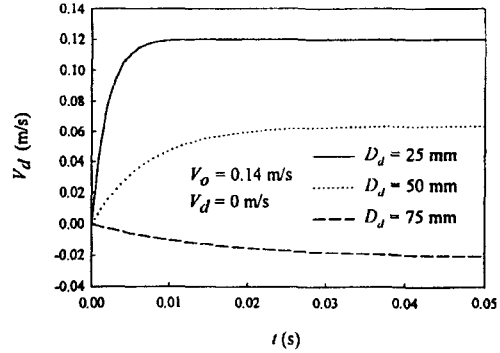


Figure 7 Droplet velocity as a function of time for three initial droplet diameters

the flame with water droplet addition than without. For low water droplet mass loading, higher air flow is required to cause blow-off. Care should be exercised when higher oxidizer flow is used because aerodynamic forces of the oxidizer may cause secondary disintegration of the liquid droplets; this will inadvertently change the droplet size distribution. The maximum velocity that can be used to establish a stable enveloped flame in our current burner is less than 2.5 m/s (based on the critical $2V_o/R$ value of 615 s^{-1}); therefore, given the droplet size used, the aerodynamic effect on secondary droplet break-up is expected to be insignificant (Bayvel and Orzechowski, 1993).

The extinction test results for the addition of nitrogen in the air stream with and without the presence of water droplets are shown in Fig. 9. The combined effect of nitrogen and water on blow-off is illustrated. With water addition, the blow-off stagnation velocity gradient is higher than that with air diluted with nitrogen. For a given nitrogen dilution, the blow-off

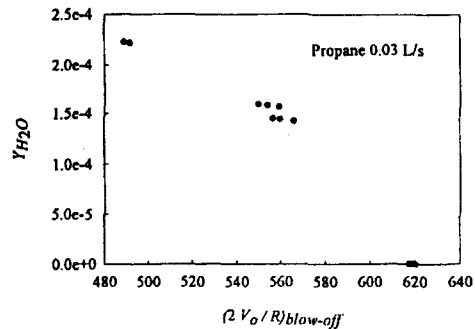


Figure 8 Mass fraction of water added in air as a function of stagnation velocity gradient at blow-off

Olson, S.L. and T'ien, J.S., "A Theoretical Analysis of the Extinction Limits of a Methane-Air Opposed-Jet Diffusion Flame," *Comb. Flame*, **70**, 161 (1987).

Peters, N. and Kee, R.J., "The Computation of Stretched Laminar Methane-Air Diffusion Flames Using a Reduced Four-Step Mechanism," *Comb. Flame*, **68**, 17 (1987).

Schneider, J.M. and Hendricks, C.D., "Source of Uniform-Sized Liquid Droplets," *Rev. Sci. Instrum.*, **35**, 1349 (1964).

Sick, V., Arnold, A., Dießel, E., Dreier, T., Ketterle, W., Lange, B., Wofrum, J., Thiele, K.U., Behrendt, F., and Warnatz, J., "Two-Dimensional Laser Diagnostics and Modeling of Counterflow Diffusion Flames," *Twenty-third Symposium (International) on Combustion*, The Combustion Institute, Pittsburgh, PA, pp. 495-501, 1990.

Tsuji, H., "Counterflow Diffusion Flames," *Prog. Energy Combustion Sci.*, **8**, 93 (1982).

Tsuji, H. and Yamaoka, I., "The Counterflow Diffusion Flame in the Forward Stagnation Region of a Porous Cylinder," *Eleventh Symposium (International) on Combustion*, The Combustion Institute, Pittsburgh, PA, pp. 979-984, 1967.

Tsuji, H. and Yamaoka, I., "The Structure of Counterflow Diffusion Flames in the Forward Stagnation Region of a Porous Cylinder," *Twelfth Symposium (International) on Combustion*, The Combustion Institute, Pittsburgh, PA, pp. 997-1005, 1969.

Tsuji, H. and Yamaoka, I., "Structure Analysis of Counterflow Diffusion Flames in the Forward Stagnation Region of a Porous Cylinder," *Thirteenth Symposium (International) on Combustion*, The Combustion Institute, Pittsburgh, PA, pp. 723-731, 1971.

Warnica, W.D., Van Reenen, M., Renksizbulut, M., and Strong, A.B., "A Piezoelectric Droplet Generator for Use in Wind Tunnels," *Rev. Sci. Instrum.*, **62**, 3037 (1991).

Yang, J.C., Chien, W., King, M., and Grosshandler, W.L., "A Simple Piezoelectric Droplet Generator," *Experiments in Fluids*, **23**, 445 (1997).